Structural Basis for AMPA Receptor Activation and Ligand Selectivity: Crystal Structures of Five Agonist Complexes with the GluR2 Ligand-binding Core

ARTICLE *in* JOURNAL OF MOLECULAR BIOLOGY · OCTOBER 2002

Impact Factor: 4.33 · DOI: 10.1016/S0022-2836(02)00650-2

doi:10.1061/S0022-2836(02)00650-2 available online at http://www.idealibrary.com on IDEAL® J. Mol. Biol. (2002) 322, 93–109

JMB

Structural Basis for AMPA Receptor Activation and Ligand Selectivity: Crystal Structures of Five Agonist Complexes with the GluR2 Ligand-binding Core

A. Hogner[1], J. S. Kastrup[1]*, R. Jin[2], T. Liljefors[1], M. L. Mayer[3] J. Egebjerg[4], I. K. Larsen[1] and E. Gouaux[2,5]*

[1]*Department of Medicinal Chemistry, Royal Danish School of Pharmacy Universitetsparken 2, DK 2100 Copenhagen, Denmark*

[2]*Department of Biochemistry and Molecular Biophysics Columbia University, 650 W 168th Street, New York, NY 10032, USA*

[3]*Laboratory of Cellular and Molecular Neurophysiology National Institute of Child Health and Human Development, National Institutes of Health, Bethesda MD 20892, USA*

[4]*Department for Molecular and Structural Biology, University of Aarhus, DK-8000 Aarhus Denmark*

[5]*Howard Hughes Medical Institute, Columbia University 650 W 168th Street, New York NY 10032, USA*

**Corresponding authors*

Glutamate is the principal excitatory neurotransmitter within the mammalian CNS, playing an important role in many different functions in the brain such as learning and memory. In this study, a combination of molecular biology, X-ray structure determinations, as well as electrophysiology and binding experiments, has been used to increase our knowledge concerning the ionotropic glutamate receptor GluR2 at the molecular level. Five high-resolution X-ray structures of the ligand-binding domain of GluR2 (S1S2J) complexed with the three agonists (*S*)-2-amino-3-[3-hydroxy-5-(2-methyl-2*H*-tetrazol-5-yl)isoxazol-4-yl]propionic acid (2-Me-Tet-AMPA), (*S*)-2-amino-3-(3-carboxy-5-methylisoxazol-4-yl)propionic acid (ACPA), and (*S*)-2-amino-3-(4-bromo-3-hydroxy-isoxazol-5-yl)propionic acid (Br-HIBO), as well as of a mutant thereof (S1S2J-Y702F) in complex with ACPA and Br-HIBO, have been determined. The structures reveal that AMPA agonists with an isoxazole moiety adopt different binding modes in the receptor, dependent on the substituents of the isoxazole. Br-HIBO displays selectivity among different AMPA receptor subunits, and the design and structure determination of the S1S2J-Y702F mutant in complex with Br-HIBO and ACPA have allowed us to explain the molecular mechanism behind this selectivity and to identify key residues for ligand recognition. The agonists induce the same degree of domain closure as AMPA, except for Br-HIBO, which shows a slightly lower degree of domain closure. An excellent correlation between domain closure and efficacy has been obtained from electrophysiology experiments undertaken on non-desensitising GluR2i(Q)-L483Y receptors expressed in oocytes, providing strong evidence that receptor activation occurs as a result of domain closure. The structural results, combined with the functional studies on the full-length receptor, form a powerful platform for the design of new selective agonists.

Keywords: glutamate receptors; X-ray structures; ligand binding; selectivity; electrophysiology

Abbreviations used: iGluRs, ionotropic glutamate receptors; mGluRs, metabotropic glutamate receptors; ACPA, (*S*)-2-amino-3-(3-carboxy-5-methylisoxazol-4-yl)propionic acid; 2-Me-Tet-AMPA, (*S*)-2-amino-3-[3-hydroxy-5-(2-methyl-2*H*-tetrazol-5-yl)isoxazol-4-yl]propionic acid; Br-HIBO, (*S*)-2-amino-3-(4-bromo-3-hydroxy-isoxazol-5-yl)propionic acid; 2-Py-AMPA, (*S*)-2-amino-3-[3-hydroxy-5-(2-pyridyl)isoxazol-4-yl]propionic acid; 3-Py-AMPA, (*RS*)-2-amino-3-[3-hydroxy-5-(3-pyridyl)isoxazol-4-yl]propionic acid; 1-Me-Imi-AMPA, (*RS*)-2-amino-3-[3-hydroxy-2-(1-methylimidazolyl)isoxazol-4-yl]propionic acid; 2-thienyl-ACPA, (*RS*)-2-amino-3-[3-hydroxy-5-(2-thienyl)isoxazol-4-yl]propionic acid; 2-Py-HIBO, (*RS*)-2-amino-3-[3-hydroxy-4-(2-pyridylisoxazol-5-yl]propionic acid; DNQX, 6,7-dinitro-2,3-quinoxalinedione; CNS, central nervous system.

E-mail addresses of the corresponding authors: jsk@dfh.dk; jeg52@columbia.edu

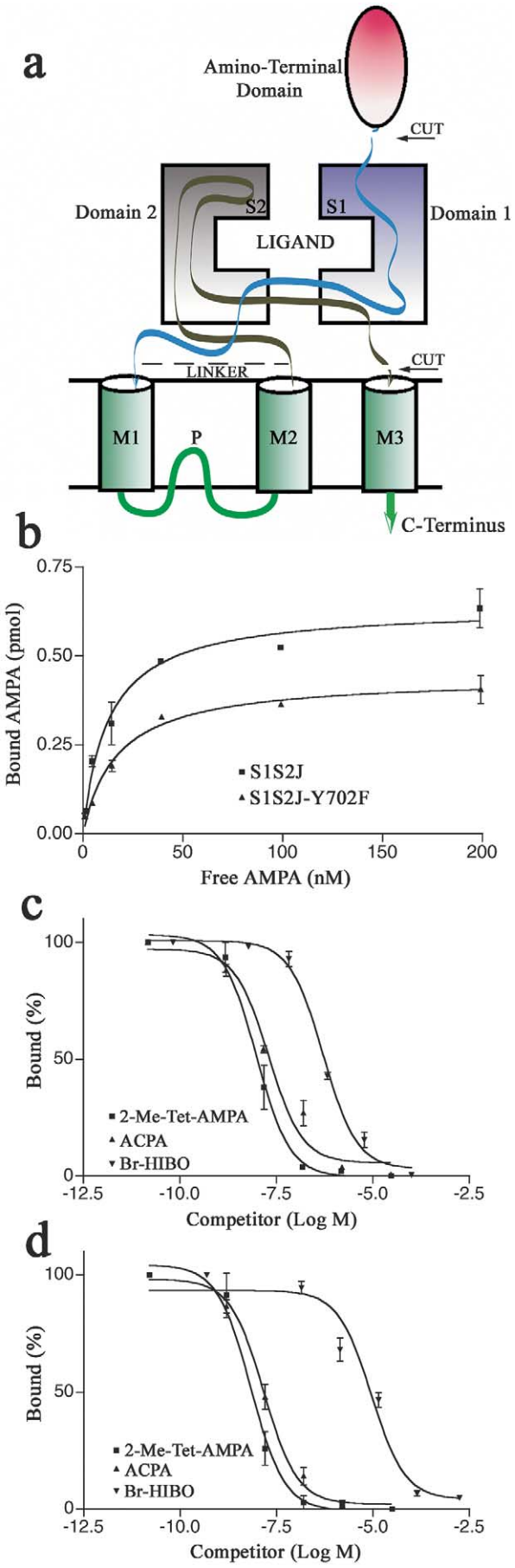

Introduction

Fast synaptic transmission in the mammalian central nervous system (CNS) is mediated primarily by glutamate receptor ion channels.[1] Glutamate receptors (GluRs) exist as ligand-gated ionotropic receptors (iGluRs) and G-protein-coupled metabotropic receptors (mGluRs). The iGluRs are further categorised into three classes, on the basis of their sensitivity to the agonists (*RS*)-2-amino-3-(3-hydroxy-5-methylisoxazol-4-yl)propionic acid (AMPA), kainic acid (KA) and *N*-methyl-D-aspartic acid (NMDA).[2] The AMPA-preferring receptors are constructed from the subunits GluR1–GluR4.[3] Subunits GluR5–GluR7 and KA1-2 are activated by kainate and form the KA receptors,[2] and NMDA-preferring receptors are formed by combinations of the seven subunits NR1, NR2A–NR2D, and NR3A and NR3B.[1] iGluRs display a broad heterogeneity due to the number of possible subunit combinations, the expression of different splice forms,[1] and post-transcriptional RNA editing.[4] This diversity gives rise to different functional properties, pharmacological profiles, and biological roles.[1,5]

On the basis of experimental studies[6–9] and sequence analyses,[10] several domains of the eukaryotic iGluR subunits have been identified. Each of the subunits (900–1400 amino acid residues) is composed of: (1) an amino-terminal domain (ATD); (2) a ligand-binding core (S1 and S2); (3) three membrane-spanning domains (M1, M2 and M3); (4) one cytoplasmic re-entrant loop (P); and (5) a C-terminal intracellular region (Figure 1(a)). The two discontinuous segments S1 and S2, responsible for binding the neurotransmitter, are related in terms of amino acid sequence and structure to the bacterial periplasmic-binding proteins.[11,12] By introducing a hydrophilic linker between the segments S1 and S2, previous studies have demonstrated the necessity and sufficiency of both segments to obtain binding affinities that are comparable with that of the full-length membrane-bound receptor.[13,14]

The development of simple and large-scale expression and purification methodologies for the

Figure 1. A representation of iGluR subunit topology and ligand binding data for S1S2J and S1S2J-Y702F. (a) The S1S2J construct comprising the ligand-binding domain of GluR2 contains S1 and S2, joined by a linker. The S1 and S2 segments are in blue and cyan, respectively. (b) K_D for [^{3}H]AMPA binding was 12.8(±1.9) nM and 17.1(±1.1) nM for S1S2J and S1S2J-Y702F, respectively. (c) IC_{50} for displacement of [^{3}H]AMPA by (*S*)-2-Me-Tet-AMPA, (*S*)-ACPA and (*S*)-Br-HIBO on S1S2J was 9.7 nM, 20.1 nM, and 0.5 μM, respectively. (d) IC_{50} for displacement of [^{3}H]AMPA by (*S*)-2-Me-Tet-AMPA, (*S*)-ACPA and (*S*)-Br-HIBO on S1S2J-Y702F was 6.9 nM, 14.8 nM, and 9.2 μM, respectively. The difference in B_{max} for S1S2J and S1S2J-Y702F is due to different protein concentrations in the experiments.

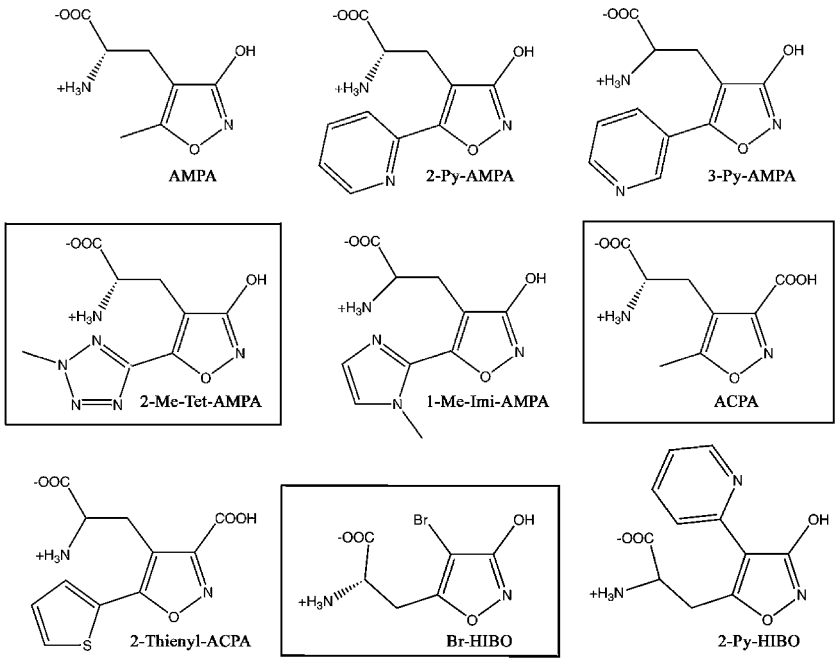

Figure 2. Chemical structures of selected AMPA receptor agonists. The three agonists that have been crystallised with S1S2J are shown within boxes.

GluR2-S1S2 constructs[14,15] have resulted in a number of high-resolution X-ray structures.[12,16] The structures in complex with AMPA, glutamate, kainate and 6,7-dinitro-2,3-quinoxalinedione (DNQX) have identified residues involved in ligand–protein interactions.[12,16] The ligands are bound in a cleft between two domains. Domain 1 is composed of segment S1 and the C-terminal end of segment S2. The C-terminal end of segment S1 ends in domain 2, which primarily is composed of segment S2. In addition, the comparison of the apo structure of GluR2-S1S2 with the above structures has revealed different degrees of domain closure induced by individual ligands, located potential subunit–subunit contact sites, and prepared the way for a proposed model for the mechanism of activation, deactivation and modulation of iGluRs.[16] Furthermore, this structural information highlighted the significant role of domain–domain interactions in determining ligand affinity and specificity, as well as kinetic properties of the channels.

The design and functional studies of new agonists and antagonists have provided important information about the structural and conformational requirements for activation and deactivation of iGluRs (for a comprehensive review, see Bräuner-Osborne *et al.*[17]). A substantial number of these ligands has been derived using AMPA as a lead structure, and some of these are shown in Figure 2. For example, the 5-methyl group has been replaced by a variety of alkyl, aryl, or heteroaryl groups. This work has resulted in a wealth of ligands displaying a broad range of activities. However, AMPA is the only isoxazole-containing ligand for which there is a structure in complex with S1S2.[16] It remains to be seen whether all AMPA agonists have the same binding modes and if differences in activities of structurally related AMPA analogues can be explained by different binding modes to the receptor.

Despite the large number of AMPA receptor agonists, very few display subtype selectivity for AMPA receptors. However, the AMPA analogue Br-HIBO has been identified as a subtype-selective agonist among AMPA receptors, differentiating the homomeric receptors GluR1o from GluR3o by a ca 70-fold difference in affinity of the racemate.[18] On the basis of binding experiments, it has been found that mutation of a single amino acid residue (Tyr698) in GluR1o to the corresponding residue in GluR3o (Phe) accounts for an 18-fold decrease in affinity for Br-HIBO.[19] Tyr698 is located in the binding site of S1S2 and corresponds to Tyr702 in GluR2o. The structural role of Tyr702 for binding of Br-HIBO is not fully understood.

Detailed structural information is crucial in order to understand the mechanism underlying ligand recognition, selectivity, and activity. Here, we report the X-ray structures of three AMPA receptor agonists with an isoxazole moiety in complex with GluR2-S1S2 (Figure 2): ACPA,[20,21] 2-Me-Tet-AMPA,[22,23] and Br-HIBO,[24,25] as well as the structures of ACPA and Br-HIBO in complex with the S1S2-Y702F mutant. The S1S2J protein has been characterised by binding experiments to verify the correct fold of the construct. Furthermore, we have performed electrophysiology experiments on oocytes expressing homomeric GluR2i receptors. The high-resolution structures of the complexes provide a decisive increase in the understanding of the receptor–ligand interactions as well as of conformational changes related to channel activation. The GluRs are associated with certain neurologic and psychiatric diseases, and are potential therapeutic targets for drugs.[17,26]

Table 1. Data collection statistics

Data set	S1S2J:ACPA	S1S2J:2-Me-Tet-AMPA	S1S2J:Br-HIBO	S1S2J-Y702F:ACPA	S1S2J-Y702F:Br-HBO
Space group	$P2_12_12$	$P2_12_12$	$P2_12_12$	$P2_12_12$	$P2_12_12$
Unit cell dimensions (Å)					
a	114.0	114.4	87.9	113.7	87.1
b	163.2	164.3	64.0	163.4	63.7
c	46.8	47.3	48.0	47.1	47.9
Crystal mosaicity (deg.)	0.15	0.42	0.69	0.26	0.54
No. per a.u.[a]	3	3	1	3	1
Wavelength (Å)	0.842	1.542	0.886	0.850	0.802
Resolution (Å)	20–1.46	20–1.85	20–1.65	20–1.95	20–1.73
Unique obs.	148,394	76,427	35,035	64,323	27,834
Average redundancy	4.2	4.4	4.2	4.3	4.8
Completeness (%)[b]	97.4 (93.9)	99.0 (91.4)	99.3 (95.1)	99.4 (98.1)	97.9 (97.4)
R_{merge} (%)[b,c]	4.5 (41.6)	6.3 (28.4)	5.6 (53.8)	7.6 (48.7)	7.2 (39.3)
$I/\sigma(I)^2$	20.8 (2.5)	19.0 (2.4)	21.7 (2.2)	11.9 (2.3)	14.3 (4.0)

[a] Number of protein molecules per asymmetric unit.
[b] Values in parentheses are statistics for the highest-resolution bin.
[c] $R_{merge}(I) = \sum_{hkl}|I_{hkl} - \langle I_{hkl}\rangle|/\sum_{hkl} I_{hkl}$, where I_{hkl} is the measured intensity of the reflections with indices *hkl*.

These studies will facilitate the design of new selective AMPA receptor agonists.

Results

High-resolution X-ray structures have been determined of the GluR2 ligand-binding domain S1S2J[16] in complex with the three isoxazole-containing agonists 2-Me-Tet-AMPA, ACPA and Br-HIBO, as well as of ACPA and Br-HIBO in complex with the S1S2-Y702F mutant (all numbering is according to the predicted mature GluR2 sequence;[27] Figure 2 and Tables 1 and 2). The S1S2J-Y702F construct was developed in order to understand the selectivity of Br-HIBO between GluR1o and GluR3o (K_i is 0.17 μM and 12.0 μM for GluR1 and GluR3, respectively).[19] The high level of sequence identity (85–90%) between S1S2 in GluR1o, GluR2o and GluR3o suggests that they will adopt the same fold. Furthermore, all amino acid residues interacting directly or through water molecules to Br-HIBO in the S1S2J complex reported here are strictly conserved, except Tyr702 (corresponding to Tyr698 in GluR1o and Phe706 in GluR3o, equivalent to Tyr716 and Phe728 as

Table 2. Refinement statistics

Data set	S1S2J:ACPA	S1S2J:2-Me-Tet-AMPA	S1S2J:Br-HIBO	S1S2J-Y702F:ACPA	S1S2J-Y702F:Br-HIBO
Resolution (Å)	20–1.46	20–1.85	20–1.65	20–1.95	20–1.73
No. atoms					
Protein	6057	6057	2019	6054	2018
Ligand	45	54	13	45	13
Water	979	1160	404	852	326
No. ions					
Zinc	8	5	0	6	0
Acetate	1	0	0	1	0
Sulphate	0	0	0	0	2
R_{work}[a]/R_{free}[b] (%)	20.2/21.6	19.6/23.4	19.2/22.1	19.2/23.0	18.6/21.4
rms deviation					
Bond lengths (Å)	0.005	0.005	0.005	0.006	0.005
Bond angles (deg.)	1.2	1.1	1.2	1.2	1.2
Mean *B*-values (Å^2)					
Overall protein	18.6	20.8	19.0	26.8	21.8
Main-chain	17.0	19.7	17.4	25.3	19.9
Side-chain	20.2	22.0	20.5	28.4	23.8
Water	31.1	34.5	32.6	39.6	39.0
Ligand	15.5	15.9	15.6	24.4	28.5
Zinc ions	24.1	29.9		33.3	
Acetate ions	30.9			46.7	
Sulphate ions					42.6
Residues in allowed regions (%)[c]	100.0	98.6	99.6	99.4	99.1

[a] $R_{work} = \sum_{hkl}||F_o| - |F_c||/\sum|F_o|$, where $|F_o|$ and $|F_c|$ are the observed and calculated structure factor amplitudes for reflection *hkl*, respectively.
[b] 10% of the reflections in the S1S2J:2-Me-Tet-AMPA, S1S2J:Br-HIBO, and S1S2J-Y702:ACPA and 5% of the reflections in the S1S2J:ACPA and S1S2J-Y702:Br-HIBO data set were set aside for calculation of the R_{free} value.
[c] The Ramachandran plots were calculated according to Kleywegt *et al.*[59]

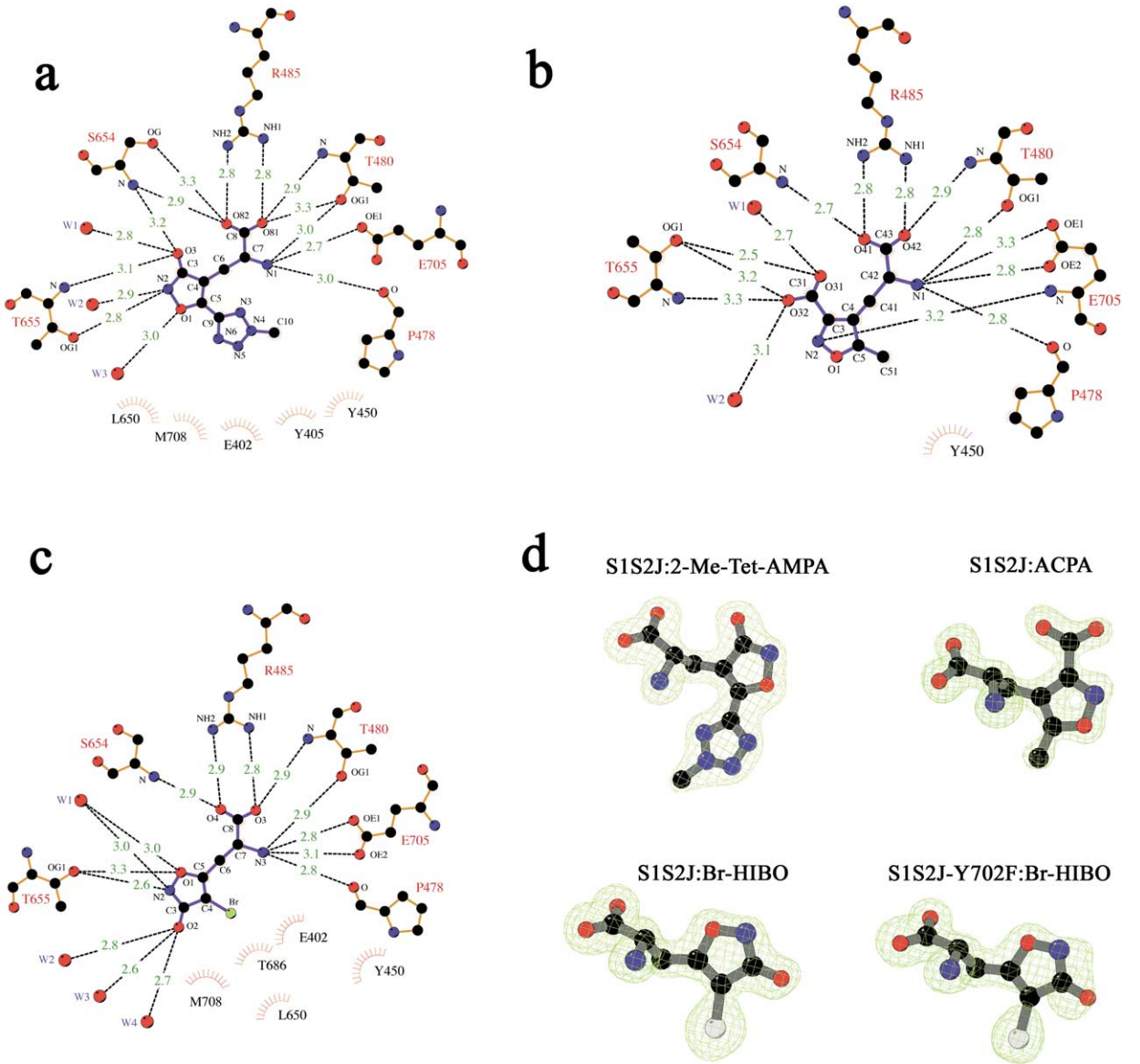

Figure 3. Drawings showing the three agonists and their interactions with the S1S2J protein. (a) 2-Me-Tet-AMPA, (b) ACPA, and (c) Br-HIBO. The bonds of the protein are displayed in yellow and the bound agonists bonds are in blue. Water molecules are shown as red spheres, while remaining atoms are in standard atomic colours (carbon is black, oxygen is red, nitrogen is blue, and bromine is green). Broken lines indicate all potential hydrogen bonds or ionic interactions within 3.3 Å. Radiating spheres indicate hydrophobic contacts within 3.9 Å between carbon atoms in the agonist and neighbouring residues. The only exception is in (c), where hydrophobic contacts between the bromine atom and neighbouring residues are displayed. The binding site of protomer A was employed for (a) and (b), and the binding sites for protomers B and C have similar structures. This Figure was prepared with the program Ligplot.[55] (d) $F_o - F_c$ omit electron density map contoured at 3.0σ for S1S2J:2-Me-Tet-AMPA, S1S2J:ACPA, S1S2J:Br-HIBO, and S1S2J-Y702F:Br-HIBO was prepared by BOBSCRIPT.[56]

labelled by Banke *et al.*[19]) and Ser652 (Ala648 in GluR1o and Ser656 in GluR3o). However, only a water-mediated backbone interaction of Ser652 with the Br-HIBO molecule is observed. Therefore, in terms of protein–ligand interactions the S1S2-Y702F construct is a good representative of the binding core of GluR3.

Ligand-binding data showed that the proteins reproduced the binding characteristics of the membrane-bound receptors,[19,21,23,25] whereas 2-Me-Tet-AMPA and ACPA displayed no selectivity for the S1S2-Y702F construct, (Figure 1(b)–(d)). However, Br-HIBO shows ca 18-fold higher affinity for the wild-type than for the mutant construct ($IC_{50} = 0.5\ \mu M$ for S1S2J and $9.2\ \mu M$ for S1S2-Y702F) as illustrated in Figure 1(c) and (d). This is in good agreement with the selectivity observed for Br-HIBO between GluR1o and GluR1o-Y698F or between the GluR3o and GluR3o-F706Y full-length receptors.[19]

The crystal structures of the 2-Me-Tet-AMPA and ACPA complexes contain three molecules in

Table 3. Potential hydrogen bonds (<3.3 Å) between S1S2J residues and water molecules that are in direct interaction with the ligands (Å)

S1S2J:2-Me-Tet-AMPA[a]		S1S2J:ACPA[a]		S1S2J:Br-HIBO	
W1–L650 O	2.7	W1–T649 OG1	3.1	W1–S652 OG	2.7
W1–G653 N	3.3	W1–L650 N	3.2	W1–T655 N	3.0
W1–G653 O	2.8	W1–Y702 OH	3.2	W1–K656 N	3.1
W1–K656 N	3.3	W1–L703 O	2.8	W2–L650 N	2.9
W2–L650 N	2.7	W2–L650 O	2.8	W2–L703 O	2.7
W2–L703 O	2.5	W2–T655 N	3.2	W3–T686 OG1	2.8
W3–T686 OG1	2.8	W2–K656 N	2.8	W3–Y702 OH	2.7
W3–Y702 OH	2.7			W4–E705 N	3.0
				W4–M708 S	3.3

[a] Protomer A was employed.

the asymmetric unit defined as A, B, and C. Only one molecule is present in the asymmetric unit of the two structures of the Br-HIBO complexes. In all complexes, two of the protein molecules form a 2-fold symmetric dimer. In the case of Br-HIBO, the two protein molecules are strictly symmetry-related. The electron density maps are of high quality for the entire protein sequence Lys393-Lys506 (S1), the Gly–Thr linker, and Pro632–Cys773 (S2). The ligands were fit into the electron density unambiguously, as shown in Figure 3(d).

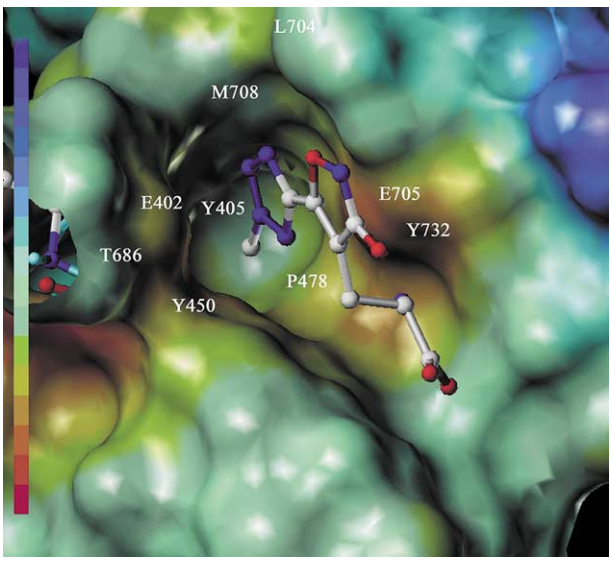

Figure 4. Surface electrostatic potential of part of the binding site of 2-Me-Tet-AMPA in complex with S1S2J. Positive potential is coloured in blue and negative potential in red, as indicated by the coloured bar to the left. The labelled residues form a well-defined partly hydrophobic and partly polar cavity within the binding site of S1S2J. These residues are within 3.9 Å from the 2-methyltetrazole ring, except from residues Thr686 and Leu704, which are at a distance of 4.2 Å and 4.7 Å, respectively. The ligand 2-Me-Tet-AMPA is shown in ball-and-stick representation, coloured as follows: carbon is white, oxygen is red, and nitrogen is blue. The Figure was prepared with the program Sybyl (Tripos Assoc. Inc.).

Interactions of the agonists with S1S2J

All three complexes include an α-carboxylate and an α-ammonium group, along with a distal anionic moiety composed of a substituted isoxazole ring. The α-carboxylate and the α-ammonium groups in all three agonists bind to S1S2J in a consistent manner. These groups form strong interactions mediated by specific hydrogen bonds and ion-pair interactions with residues from domains 1 and 2 (Figure 3(a)–(c)). The α-carboxylate group makes extensive interactions with Arg485, as well as with the backbone NH group of Ser654 and Thr480. The α-ammonium group is locked in a tetrahedral hydrogen bond network with the hydroxy oxygen atom of Thr480, the carboxylate oxygen atoms of Glu705, and the backbone carbonyl oxygen atom of Pro478.

In contrast with the conserved binding pattern for the α-substituents, variable binding orientations are observed for the isoxazole rings. The isoxazole hydroxy group of 2-Me-Tet-AMPA interacts directly with the backbone NH groups of Ser654 and Thr655, but is also linked to the protein *via* water molecule W1 (Figure 3(a) and Table 3). Similarly, the isoxazole nitrogen atom interacts directly with the hydroxy group of Thr655, and with the protein through water molecule W2. W3 mediates one additional interaction, between the furan-like isoxazole oxygen atom and the side-chain oxygen atom of Tyr702. The two heterocyclic rings of 2-Me-Tet-AMPA are co-planar. Despite the fact that the 2-methyltetrazole ring contains three basic nitrogen atoms, none of them is involved in hydrogen-bonding interactions with the protein. Instead, this ring is located between the residues Glu402, Tyr405, Tyr450, and Pro478 of domain 1 and Thr686, Leu704, Glu705, Met708, and Tyr732 of domain 2. These residues create a well-defined, partly hydrophobic and partly polar cavity as depicted in Figure 4. The shape complementarity, and the resulting favourable van der Waals interactions between the 2-methyltetrazole heterocycle and the protein, contribute to the high affinity of S1S2J for 2-Me-Tet-AMPA (IC_{50} = 10 nM).

The isoxazole rings of ACPA and 2-Me-Tet-AMPA interact in dissimilar fashions with the receptor

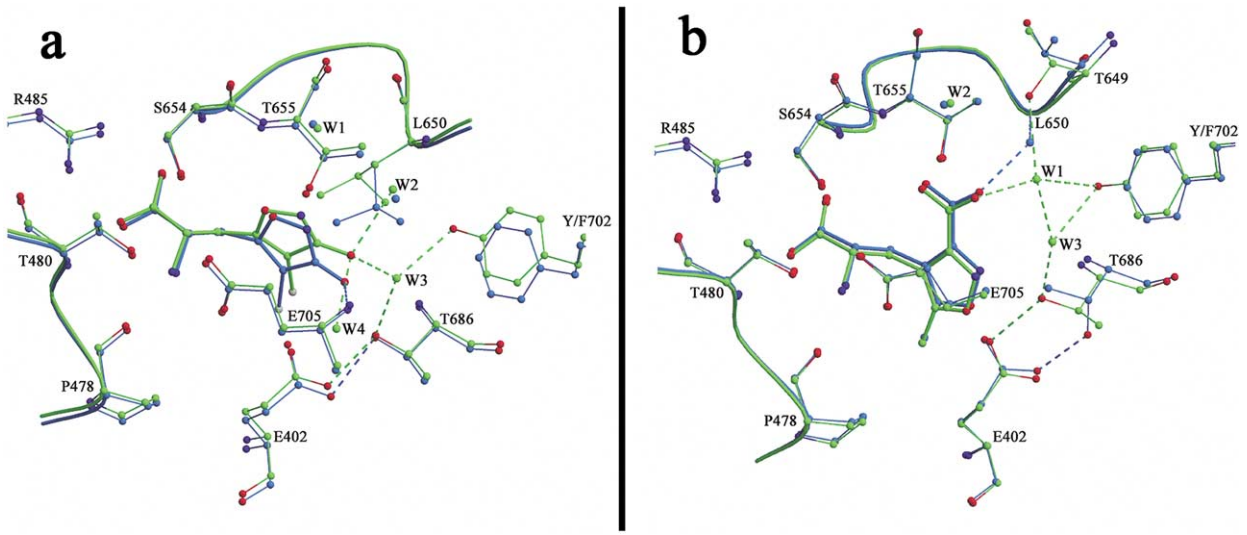

Figure 5. Comparison of the binding modes of Br-HIBO and ACPA to S1S2J and S1S2J-Y702F. (a) The structure of S1S2J:Br-HIBO superimposed onto the structure of S1S2J-Y702F:Br-HIBO. (b) The structure of S1S2J:ACPA superimposed onto the structure of S1S2J-Y702F:ACPA. Superpositions are on all C^{α} atoms. Backbone, selected side-chains, and ligands are in green and blue for S1S2J and S1S2J-Y702F complexes, respectively. Oxygen atoms are displayed in red, nitrogen in blue, and bromine in grey. Water molecules corresponding to the structures of S1S2J and S1S2J-Y702F are shown as green and blue spheres, respectively. Unique hydrogen bonds, differing between the two structures, are indicated by broken lines (green lines between ligand and S1S2J, and blue between ligand and S1S2J-Y702F). The Figure was prepared with the programs MOLSCRIPT[57] and Raster3D.[58]

(Figure 3(b)). Instead of a deprotonated 3-hydroxyisoxazole as a carboxylate bioisostere, ACPA has a carboxylate group playing the role of the distal anionic group. This carboxylate group interacts with the backbone NH group and the side-chain hydroxy group of Thr655. Furthermore, the carboxylate group is linked to the protein *via* two water molecules, W1 and W2 (Table 3). The binding of the isoxazole is further stabilised by a long hydrogen bond between the NH group of Glu705 and the isoxazole nitrogen atom. The methyl group at the 5-position of the isoxazole ring of ACPA is directed towards the pocket in which the 2-methyl-tetrazole of 2-Me-Tet-AMPA binds. However, the methyl group does not protrude as deeply into the pocket as the 2-methyltetrazole ring. Instead, it is positioned in the upper part of the pocket, where it makes hydrophobic contacts with Tyr450 and Pro478.

The binding mode of the Br-HIBO isoxazole moiety is quite different from that of the corresponding rings in 2-Me-Tet-AMPA and ACPA in terms of direct interactions with the protein (Figure 3(c)). The hydroxy group of Thr655 makes one close interaction with the isoxazole nitrogen atom and one relatively long hydrogen bond to the isoxazole oxygen atom. No further direct interaction is observed between the heterocycle and the protein. Instead, the isoxazole is involved in water-mediated hydrogen bonds to the receptor (Table 3). The oxygen and nitrogen atoms of the isoxazole interact with water molecule W1. In addition, the hydroxy group of the isoxazole is anchored in a triangular hydrogen bond pattern to water molecules W2, W3, and W4. Interestingly, the bromine atom at the 4-position of the isoxazole ring does not point directly at the pocket accommodating the 5-substituent in 2-Me-Tet-AMPA, but is positioned near the carboxylate group of Glu402 and the hydroxy group of Thr686. These two residues, which are located in domains 1 and 2, respectively, interact *via* a hydrogen bond and form a tight interaction between the two domains. Furthermore, the bromine atom is in van der Waals contacts with Tyr450, Leu650, Met708, and water molecules W3 and W4. These relatively short distances around the bromine atom (3.3–3.5 Å) are close to the acceptable van der Waals separation.

Interactions of the agonists Br-HIBO and ACPA with S1S2J-Y702F

In order to understand how the residue at position 702 influences the selectivity of the receptor for Br-HIBO, we selected ACPA for use as a reference structure because ACPA did not display any selectivity between the two constructs in the binding assay. The structural features of the α-substituents (carboxylate and ammonium groups) in the Br-HIBO and ACPA S1S2J-Y702F complexes overlap completely when compared to the corresponding S1S2J complexes (Figure 5(a) and (b)).

The electron density of the S1S2J-Y702F:Br-HIBO complex clearly shows the mutated side-chain and reveals a significant conformational change of Leu650. The side-chain of Leu650 has adopted a different rotamer, which orients the methyl groups further away from the binding core. The isoxazole ring is tilted relative to its conformation in the wild-type S1S2J:Br-HIBO complex (Figure 5(a)),

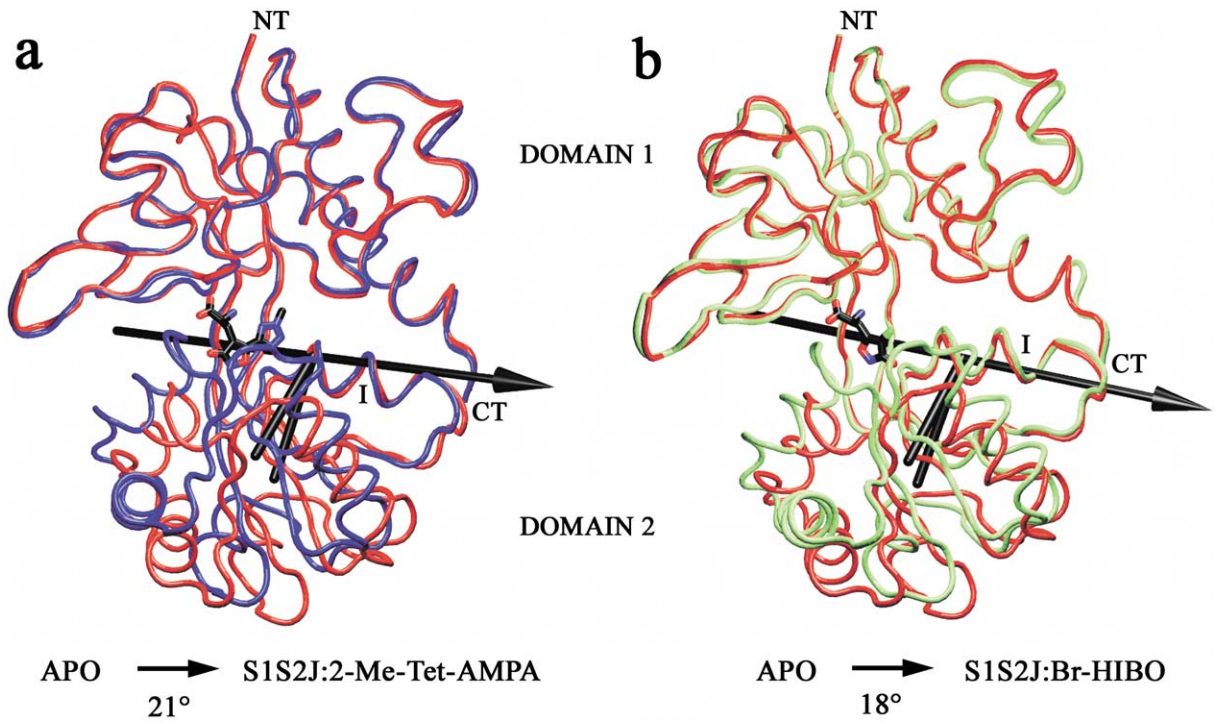

Figure 6. Domain movements of S1S2J:2-Me-Tet-AMPA and S1S2J:Br-HIBO structures, relative to the ApoA structure of S1S2J. (a) Superposition of the C^{α} trace of ApoA (red) and 2-Me-Tet-AMPA (blue) structures. (b) Superposition of the C^{α} trace of ApoA (red) and Br-HIBO (green). The calculated degree of domain closure is listed below the structures. The location of the rotation axis suggests that domain 2 moves as a rigid body relative to domain 1, except for helix I of domain 1. Prior to the calculation of the relative degree of domain closure induced by the agonists, the agonist complex structure was superimposed onto the ApoA structure, using only C^{α} atoms from domain 1 in program O.[51] The Figure was prepared with the program VMD.[29]

positioning the bromine atom closer to the opening of the well-defined pocket. A striking feature is the complete disruption of the hydrogen bond architecture involving the isoxazole hydroxy group of the S1S2J complex. There is no electron density for water molecules W3 or W4 in $2F_o - F_c$ and $F_o - F_c$ maps contoured at 0.5 and 2.0σ, respectively, suggesting that the solvent that occupies these sites transiently is now disordered. The disruption of ligand–solvent interactions is compensated partly by a long hydrogen bond (3.3 Å) between the isoxazole hydroxy group and the backbone NH of Glu705. However, the isoxazole nitrogen and oxygen atoms in the S1S2J-Y702F complex still make the same interactions as in the S1S2J complex. This decreased stabilisation of the isoxazole of Br-HIBO in the S1S2J-Y702F complex is reflected in the *B*-values and in a less well-defined electron density for the isoxazole moiety (Figure 3(d)). The *B*-values range from ca 15 $Å^2$ for the α-carboxylate group up to ca 45 $Å^2$ for the bromine atom, which is substantially higher than for the rest of the structure, indicating a higher degree of mobility of the isoxazole ring compared to the α-substituents (carboxylate and ammonium groups). By contrast, the same atoms in Br-HIBO bound to wild-type S1S2J have *B*-values that range from 12–19 $Å^2$.

ACPA is bound to S1S2J-Y702F in a manner essentially identical with the manner in which it is bound to wild-type S1S2J (Figure 5(b)). Nevertheless, notable conformational rearrangements are observed for both Thr649 and Thr686. In both cases, the side-chains have adopted another rotamer such that the CH_3 groups are facing the hydrophobic Phe702. A consequence of this new hydrophobic surface is the disruption of the adjacent water molecule network. In the S1S2J:ACPA complex, two water molecules mediate a hydrogen bond network between the isoxazole carboxylate group in ACPA and the hydroxy groups of Thr686 and Tyr702 (Figure 5(b)). This water architecture is not present in the S1S2J-Y702F complex. Instead, a water-mediated hydrogen bond is formed between the isoxazole carboxylate group in ACPA and the backbone NH group of Leu650.

Structure comparisons and domain movements

The structures of the five complexes exhibit the same fold. Pairwise superpositions of the 11 independent protein molecules in the complexes with 2-Me-Tet-AMPA, ACPA, and Br-HIBO yield root-mean-square deviations of 0.14–0.76 Å on all C^{α} atoms. The most striking conformational difference among the structures is the conformational

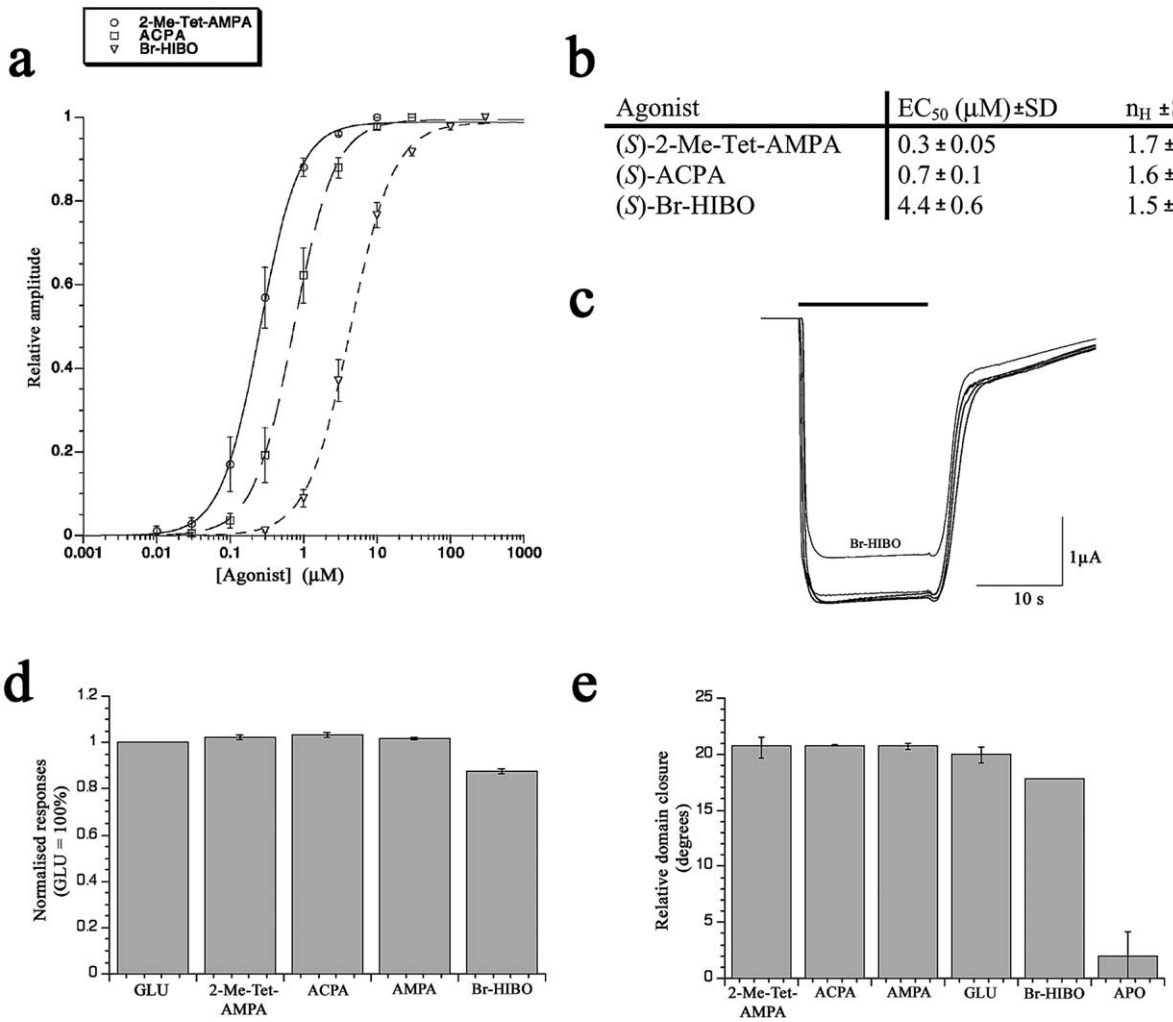

Agonist	EC_{50} (μM) ±SD	n_H ±SD
(*S*)-2-Me-Tet-AMPA	0.3 ± 0.05	1.7 ± 0.1
(*S*)-ACPA	0.7 ± 0.1	1.6 ± 0.1
(*S*)-Br-HIBO	4.4 ± 0.6	1.5 ± 0.1

Figure 7. Pharmacological profiles of (*S*)-2-Me-Tet-AMPA, (*S*)-ACPA, (*S*)-Br-HIBO, (*S*)-AMPA, and (*S*)-Glu at GluR2i(Q)-L483Y homomeric receptor using two electrode voltage clamping in Xenopus oocytes, in comparison with the ligand-induced domain closure of S1S2J. (a) Dose-response curves of 2-Me-Tet-AMPA, ACPA, and Br-HIBO on homomeric GluR2i(Q)-L483Y receptor expressed in Xenopus oocytes (normalised to 1 for the purpose of illustration). Five oocytes per agonist were used in total and one to two EC_{50} values were determined for each oocyte. Standard deviation (SD) values are indicated as error bars. (b) EC_{50} and Hill coefficient values were calculated from the dose-response curves in (a), using the equation:

$$I = I_{max}/[1 + (EC_{50}/[\text{agonist}])^n]$$

where I_{max} is the response at a saturating concentration of ligand, EC_{50} is the concentration of ligand producing a half-maximal response, and n is the Hill coefficient. Values are the means ± SD. (c) Representative superimposed traces evoked by saturating concentrations (bar) of 2-Me-Tet-AMPA (30 μM), ACPA (100 μM), Br-HIBO (500 μM), AMPA (600 μM), and Glu (2 mM), recorded from one oocyte. A markedly lower efficacy for Br-HIBO is observed. (d) Comparison of the agonist efficacy of 2-Me-Tet-AMPA, ACPA, Br-HIBO, AMPA, and Glu at GluR2i(Q)-L483Y homomeric receptors. Whole-cell responses evoked by saturating concentrations of the agonists were recorded from five oocytes per agonist. Peak responses from the agonists were normalised to the response elicited by 2 mM glutamate (EC_{50} 20 μM, N. Armstrong, M.L.M, & E.G., unpublished results). Values are the means ± SD. (e) Plots of the mean domain closure of S1S2J:2-Me-Tet-AMPA, S1S2J:ACPA, S1S2J:Br-HIBO, S1S2J:AMPA, and S1S2J:Glu, relative to the ApoA structure.[16] Error bars indicate the minimum and maximum domain closure values found for the molecules in the asymmetric unit.

variability in the orientation of the two domains. An analysis of the differences in domain positioning for each structure relative to the apo structure of S1S2J (ApoA, PDB ID code 1FTO[16]) was performed using the HINGEFIND script[28] implemented in the program VMD.[29] This resulted in the partitioning of the protein into two rigid-body domains, corresponding approximately to domains 1 and 2 in the two constructs. Binding of 2-Me-Tet-AMPA and ACPA to S1S2J induces ca 21° of domain closure around an axis between the domains, oriented along helix I, as illustrated in Figure 6(a). A slight difference in the degree of domain closure was observed for the different

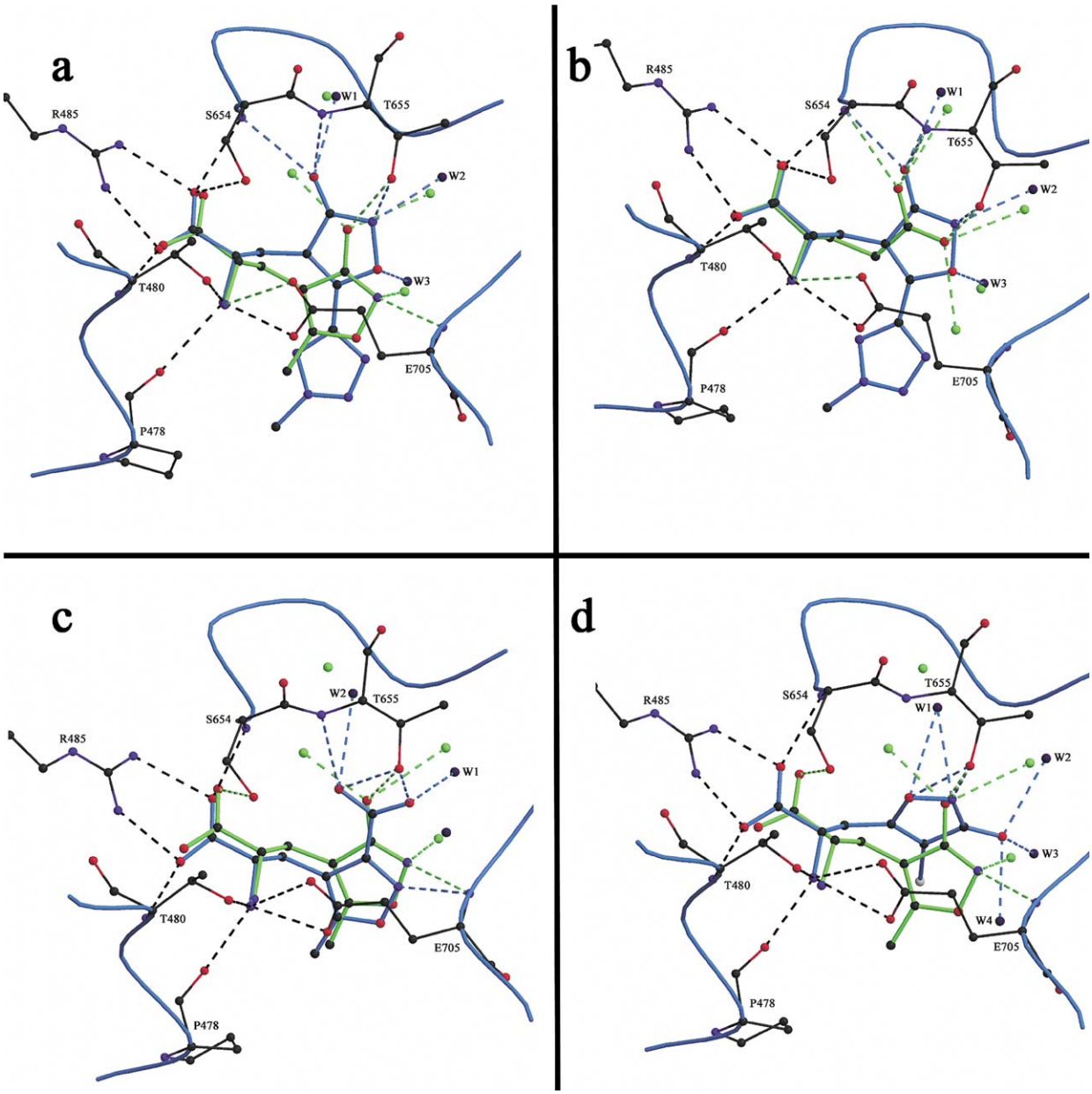

Figure 8. A comparison of the binding modes of (*S*)-2-Me-Tet-AMPA, (*S*)-ACPA, (*S*)-Br-HIBO, (*S*)-AMPA, and (*S*)-glutamate within the ligand-binding site of S1S2J. (a) The structure of 2-Me-Tet-AMPA superimposed onto the structure of AMPA. (b) The structure of 2-Me-Tet-AMPA superimposed onto the structure of glutamate. (c) The structure of ACPA superimposed onto the structure of AMPA. (d) The structure of Br-HIBO superimposed onto the structure of AMPA. For the 2-Me-Tet-AMPA, ACPA, AMPA, and glutamate complexes, protomer A was used for superpositions using all C^{α} atoms. The conformations of Pro478, Thr480, Arg485, Ser654, Thr655 and Glu705 are conserved in all molecules and only the backbone (light blue) and side-chains (atom coloured) of the reported structures are shown. Bonds in 2-Me-Tet-AMPA, ACPA, and Br-HIBO are in light blue and atoms are in standard atomic colours (carbon in black, oxygen in red, bromine in grey, and nitrogen in blue). Water molecules corresponding to the structures of 2-Me-Tet-AMPA, ACPA, and Br-HIBO are shown as blue spheres. AMPA and glutamate with corresponding water molecules are coloured green. Conserved hydrogen bonds between ligands and S1S2J within 3.3 Å of the superimposed structures are indicated by broken black lines. Unique hydrogen bonds within 3.3 Å are in light blue for 2-Me-Tet-AMPA, ACPA, and Br-HIBO, respectively, and in green for AMPA and glutamate, respectively. The Figure was prepared with the programs MOLSCRIPT[57] and Raster3D.[58]

molecules in the asymmetric unit of 2-Me-Tet-AMPA (20–21°) and may be due to lattice contacts. However, Br-HIBO binding to S1S2J induces a domain closure of ca 18°, significantly less than 2-Me-Tet-AMPA and ACPA. Moreover, the orientation of the axis describing the domain closure in the Br-HIBO structure is positioned closer to domain 2 compared to the axis found in the case of the 2-Me-Tet-AMPA and ACPA complexes (Figure 6(b)). No significant difference in domain closure was observed

for Br-HIBO (ca 0.4°) and ACPA (ca 1°) bound to S1S2J-Y702F compared to S1S2J.

The differences in domain closure between 2-Me-Tet-AMPA and ACPA on the one hand, and Br-HIBO on the other, considerably influence the conformations of backbone between Asp651 and Gly653. This peptide segment adopts approximately the same conformation in both molecules of the two Br-HIBO complexes. However, in all nine molecules in the asymmetric units of the three complexes with 2-Me-Tet-AMPA and ACPA the *trans* peptide bond between Asp651 and Ser652 has flipped ca 180°. Interestingly, in the Br-HIBO structures, the carbonyl backbone oxygen atom of Ser652 is involved in water-mediated interactions to the oxygen and nitrogen atoms in the Br-HIBO isoxazole moiety. In the 2-Me-Tet-AMPA and ACPA complexes, neither of the two residues is involved in ligand interactions.

Ion channel activities and pharmacological profile of the ligands

In order to investigate the functional consequences of differences in domain closure, two electrode voltage clamp experiments were performed on GluR2i(Q)-L483Y receptors expressed in Xenopus oocytes. The point mutation L483Y greatly reduces desensitisation and makes it possible to record peak currents elicited upon agonist application.[30] Oocytes expressing homomeric GluR2i-L483Y receptors responded reproducibly to bath applications of the ligands. As shown in Figure 7(a) and (b), the observed rank order of potency (EC_{50}) was: 2-Me-Tet-AMPA (0.26 μM) > ACPA (0.74 μM) > Br-HIBO (4.38 μM), and is in full agreement with the potencies measured from electrophysiology recordings on oocytes expressing GluR1o homomeric receptors.[19,23,31] The Hill coefficients were between 1.5 and 1.7 for all ligands tested. The efficacy was examined by measuring the currents elicited by saturating concentrations of 2-Me-Tet-AMPA, ACPA and Br-HIBO, using AMPA and Glu as references. Interestingly, all ligands displayed very similar amplitude currents, except for Br-HIBO. The marked difference in the efficacy of Br-HIBO is illustrated in Figure 7(d), where Br-HIBO currents are only 85% of full agonist currents. Interestingly, Br-HIBO also induces only ca 85% of domain closure compared to full agonists (Figure 7(e)).

Discussion

Ionotropic glutamate receptors exhibit a complex molecular pharmacology that has been exploited by the generation of a large number of competitive full agonists, partial agonists and antagonists. While the number and diversity of glutamate receptor structure–activity studies are impressive, there has been no firm structural basis on which to ground an understanding of the basis for ligand–receptor selectivity. The five high-resolution X-ray structures reported here, combined with the electrophysiology and binding experiments, provide a detailed insight into the molecular mechanisms that constitute the initial events of receptor activation.

Agonist-binding modes to S1S2J

Superpositions of the structures of the ligand-binding core of GluR2 (S1S2J) in complex with the various agonists (the three reported here as well as glutamate, AMPA and kainate[16]) show that the fundamental interactions between the receptor and both the α-carboxylate group and the α-ammonium group of the agonists are conserved. The crucial difference between 2-Me-Tet-AMPA and AMPA bound to S1S2J lies in the different positioning of the isoxazole rings. Compared to the isoxazole in AMPA, the isoxazole in 2-Me-Tet-AMPA is situated considerably closer to domain 2 (Figure 8(a)). In this position, the isoxazole hydroxy group replaces a water molecule in the S1S2J:AMPA structure and makes two additional and direct protein interactions that are not found in the complex with AMPA.

On the basis of studies of a large number of AMPA analogues having different substituents at the 5-position of the isoxazole ring, it has been proposed that AMPA receptors contain a cavity that can accommodate lipophilic substituents up to a certain size.[32] The crystal structures disclose such a well-defined pocket within the binding site (Figure 4). In addition, the size and shape of the 5-substituent determine the binding position of the isoxazole ring. This means that AMPA analogues with bulky groups at the 5-position will adopt a 2-Me-Tet-AMPA-binding mode, as the substituents otherwise will interfere sterically with the residues forming the cavity. On the basis of the 2-Me-Tet-AMPA complex, it is evident that the 2-methyltetrazole group fits the pocket perfectly. Compared to 2-Me-Tet-AMPA, agonists with bulkier groups in the 5-position do not approach the potency of 2-Me-Tet-AMPA.[22,33,34] Because of the shape of the pocket, binding of bulkier groups requires shifts in the isoxazole position as well as adjustments in the positioning of side-chains and water molecules.

The hydroxy group on the 2-Me-Tet-AMPA isoxazole ring and the nitrogen atom in the ring superimpose on the distal carboxylate group of glutamate. However, the isoxazole ring of 2-Me-Tet-AMPA adopts a quite different binding mode compared to the isoxazole of AMPA (Figure 8(a) and (b)). The question arises: what is the driving force behind the different positioning observed for the isoxazole rings, of 2-Me-Tet-AMPA and AMPA? The introduction of a large 5-substituent as the tetrazole of 2-Me-Tet-AMPA leads to a five-fold decrease in the IC_{50} value compared to AMPA.[23] This decrease may be explained primarily by a favourable hydrophobic effect, due to an entropy gain upon the release of ordered water

and the binding of the tetrazole group within the partly hydrophobic pocket. The altered position of the isoxazole of AMPA, compared to 2-Me-Tet-AMPA, is most likely caused by the positioning of the 5-methyl group towards the pocket, as well as by the ability to form a similar pattern of hydrogen bonds. However, as glutamate adopts the 2-Me-Tet-AMPA-binding mode, this is probably the energetically most favourable way of binding a moiety with hydrogen bond-accepting properties of a carboxylate group. Despite the different positioning of AMPA as compared to glutamate and 2-Me-Tet-AMPA, a similar number of hydrogen bonds are formed to the distal carboxylate group of glutamate and to the 3-hydroxy isoxazole anion of AMPA and 2-Me-Tet-AMPA, respectively.

The binding orientation of the ACPA isoxazole is very similar to that observed in AMPA (Figure 8(c)). However, the rings are not superimposed completely and the ACPA isoxazole is positioned slightly closer to domain 1. When the isoxazole ring is in the ACPA position, the distal carboxylate group makes a direct interaction to the backbone NH group of Thr655 as compared to the hydroxy group in AMPA. However, the nitrogen atom in the ACPA isoxazole has also lost one potential hydrogen bond to a water molecule that is present in the AMPA structure.

It has been proposed that when Br-HIBO binds to the receptor the isoxazole ring is flipped relative to the isoxazole ring of AMPA.[19,24,35,36] However, until now experimental evidence for the specific nature of the binding of Br-HIBO compared to AMPA has been lacking. The structure of the Br-HIBO complex confirms the flipped orientation of the isoxazole ring and shows that the nitrogen atom in the Br-HIBO isoxazole replaces the hydroxy group of AMPA. The hydroxy group of Br-HIBO occupies a site similar to that of the nitrogen atom in the AMPA isoxazole (Figure 8(d)). However, the 4-bromine atom of Br-HIBO is not situated at the same site as the 5-methyl group of AMPA. This means that the bromine atom does not protude into the pocket, but is stabilised by numerous van der Waals and hydrogen-bonding interactions. This position seems to be more suitable for the bromine atom and thereby plays a decisive role in the mode of binding of this agonist.

To summarise the observed ligand interactions, the overall electrostatic interactions (charge–charge and hydrogen bonds) vary between the three complexes but the total number of interactions made by each ligand is quite consistent (14–15 hydrogen bonds per ligand). Favourable van der Waals interactions contribute to the overall strength of the binding and, together with electrostatic interactions, seem to direct the orientation of the compounds.

Agonist-binding modes to S1S2J-Y702F

The decreased affinity of Br-HIBO to S1S2J-Y702F can be explained by the disruption of the water architecture stabilising the Br-HIBO isoxazole in S1S2J. The importance of the water molecules in binding of Br-HIBO was proposed by Banke *et al.*[19] The destabilisation is reflected in the *B*-values, which are much higher for the isoxazole part of the ligand compared to the α-substituents (carboxylate and ammonium groups). Interestingly, a reorientation of the side-chain of Leu650 compensates partly for the loss of interactions to bound water molecules by adopting a rotamer with favourable interactions to Br-HIBO. The same rotamer is seen in the complex between the partial agonist kainate in complex with S1S2J. This indicates that the side-chain of Leu650 is flexible and plays an important role in accommodating ligands and in supporting subtype specificity, as the binding mode of Br-HIBO to the Y702F mutant probably mimics the binding of Br-HIBO to GluR3.

ACPA retains all direct interactions to the protein in the S1S2J-Y702F complex compared to S1S2J (Figure 5(b)). The surrounding region of Phe702 is turned into a more hydrophobic environment due to the rearrangements of Thr649 and Thr686 side-chains. The rearrangement of the Thr686 side-chain has a double effect upon binding of ACPA. Firstly, the hydrophobic CH_3 group is now facing the mutated residue Phe702. Secondly, Thr686 can still make strong interactions to Glu402, which seems to be an important allosteric interaction, stabilising the relative orientation of the two domains, as discussed below.

Binding modes of other AMPA agonists

On the basis of the agonist-binding modes revealed by our structural studies of complexes of S1S2J, several AMPA analogues have been modelled into the binding site of S1S2J. The agonist potency of AMPA analogues has been shown to decrease when the size and lipophilicity of the ring substituent in the 5-position is increased.[22,33,34] One exception is (*S*)-2-amino-3-[3-hydroxy-5-(2-pyridyl)isoxazol-4-yl]propionic acid (2-Py-AMPA) (Figure 2), a potent AMPA receptor agonist ($IC_{50} = 0.57\ \mu M$).[37] Compared to 2-Py-AMPA, (*RS*)-2-amino-3-[3-hydroxy-5-(3-pyridyl)isoxazol-4-yl]propionic acid (3-Py-AMPA) is a very weak AMPA receptor agonist ($IC_{50} > 100\ \mu M$).[34] From the structure of the 2-Me-Tet-AMPA complex, it is evident that AMPA analogues with bulky 5-substituents will adopt a 2-Me-Tet-AMPA-binding mode. This assumption was used in docking of 2-Py-AMPA and 3-Py-AMPA into the structure of the 2-Me-Tet-AMPA complex. Interestingly, the nitrogen atom in the 3-position is positioned close to Glu402 and Thr686. The proximity of the three nitrogen atoms to the side-chains of Glu402 or Thr686 may prevent domain closure and result in an unfavourable binding position. However, the nitrogen atom in the 2-position is not close to either Glu402 or Thr686. Instead, it might be possible for the nitrogen atom in the 2-position to make favourable interactions, directly or through a water

molecule, to the backbone NH group of Glu705, or alternatively make intramolecular interactions with the α-ammonium group in 2-Py-AMPA. The inactivity of (*RS*)-2-amino-3-[3-hydroxy-2-(1-methylimidazolyl)isoxazol-4-yl]propionic acid (1-Me-Imi-AMPA) ($IC_{50} > 100$ μM, Figure 2) can be attributed to the size of the 5-substituent of the isoxazole, which is too bulky to be accommodated in a closed domain conformation of S1S2J.[22]

A replacement of the 5-substituent in ACPA by a 2-thienyl ring results in an inactive compound, (*RS*)-2-amino-3-[3-hydroxy-5-(2-thienyl)isoxazol-4-yl]propionic acid (2-thienyl-ACPA) ($IC_{50} > 100$ μM, Figure 2).[38] Modelling studies based on the 2-Me-Tet-AMPA structure indicate that the carboxylate group on the isoxazole of 2-thienyl-ACPA interferes sterically with Ser654 and Thr655. Thus, ACPA analogues with bulky substituents at the 5-position will probably not be high-affinity agonists.

Introduction of aromatic substituents in the 4-position of the isoxazole ring in HIBO analogues decreases the effect at the AMPA receptors dramatically. However, (*RS*)-2-amino-3-[3-hydroxy-4-(2-pyridylisoxazolyl-5-yl]propionic acid (2-Py-HIBO) ($IC_{50} = 1.34$ μM, Figure 2) is a potent AMPA receptor agonist.[39] From the Br-HIBO structure, it is clear that HIBO analogues with larger groups than a bromine atom or a methyl group at the 4-position will direct the 4-substituent towards the partly hydrophobic pocket in a manner similar to that of the tetrazole group in 2-Me-Tet-AMPA. The 4-substituent of 2-Py-HIBO can be well accommodated in the closed conformation of S1S2J. Furthermore, the nitrogen atom in the 2-position might interact in a fashion analogous to that of the nitrogen atom in the 2-pyridyl ring of 2-Py-AMPA.

Domain closure triggers activation of AMPA receptors

Conformational changes involving rotation of domains induced by binding of ligands are a recurring, functionally important feature of a variety of proteins. This is observed also in the ligand-binding core of GluR2. It has been reported that Asn721 in GluR6 (equivalent to Thr686 in GluR2) controls both AMPA sensitivity and the domoate deactivation rate.[40] Recently, the crystal structures of various GluR2-S1S2J complexes revealed agonist-induced domain closure and that Thr686 of domain 2 interacts with Glu402 of domain 1 by hydrogen bonding in all agonist complexes but not in the open state antagonist or apo structures.[12,16] Therefore, this interaction between domains 1 and 2 of S1S2J seems to be of importance for the stabilisation of the closed conformation of the protein.

Interestingly, in the S1S2J:Br-HIBO complex, the ligand induces significantly less domain closure (18°) than in S1S2J:2-Me-Tet-AMPA and S1S2J:ACPA (21°), relative to the ApoA structure.[16] In the S1S2J:Br-HIBO structure, the bromine atom points directly at Glu402. This close approach of the bromine atom to the carboxylate group of Glu402 forces the torsion angle (C^{β}–C^{γ}–C^{δ}–$O^{\varepsilon 1}$) to an eclipsed conformation (−123°). A *gauche* conformation (ca −80°) is observed in the S1S2J:2-Me-Tet-AMPA and S1S2J:ACPA complexes, whereas the torsion angle in the complex with the partial agonist kainate is −160°. Thus, the Glu402 side-chain in the S1S2J:Br-HIBO structure has adopted a conformation between the conformations observed in the kainate structure and the 2-Me-Tet-AMPA/ACPA structures. The partial agonist kainate induces only ca 12° of domain closure and this has been explained by steric hindrance between the isopropenyl group of kainate and Leu650 in domain 2.[16] The antagonist DNQX induces only ca 5° of domain closure, which has been accounted for by blocking the interdomain Glu402–Thr686 interaction completely.[16] Furthermore, even though Br-HIBO binds with 18-fold decreased affinity to the mutant S1S2J-Y702F, it still produces the same degree of domain closure. Taken together, these results demonstrate that the degree of domain closure is regulated by steric hindrance between the two domains and/or modification of the Glu402–Thr686 interaction, and is independent of the affinity of the ligand.

The peptide segment Asp651–Gly653 has been shown to undergo a rearrangement of the backbone upon the transition from the open state (apo) to the fully closed state (e.g. AMPA).[16] Agonists can be divided into two groups with respect to the peptide conformation, except for glutamate, which induces multiple conformations. The first group consists of the three high-affinity agonists 2-Me-Tet-AMPA, ACPA, and AMPA which all induce full domain closure relative to the apo structure. The second group consists of the lower-affinity agonists Br-HIBO and KA, as well as the antagonist DNQX, which all stabilise the unflipped conformation and induce less domain closure. The peptide segment is located just before the two key residues Ser654 and Thr655, which are involved in ligand interactions; however, none of the residues involved in the peptide flip is in direct contact with the ligands. In all structures, the rearrangement generates two new interdomain hydrogen bonds (Gly451 to Ser652 and Tyr450 to Asp651 *via* a water molecule), inducing further stabilisation of the closed domains.

It has been reported that the ligand-induced conformational changes observed for the S1S2J structures as well as for the structures of the ligand-binding domain of GluR0 cause the ion channel to open.[16,41,42] This concept has been further supported from the correlation between the agonist-induced domain-closure resulting in an increase in the separation between the two molecules forming the dimer and the ability to open the channel.[42] Upon binding of the various agonists, the distance between the C^{α} atoms of e.g. Ile633 in each molecule is ca 35.7 Å for 2-Me-Tet-AMPA, ACPA, and AMPA and 34.5 Å for Br-HIBO. Agonists, which

induce a high degree of domain closure, lead to a larger separation between the two C^{α} atoms compared to agonists that do not induce full closure. Ile633 is adjacent to the Gly–Thr linker and proximal to the transmembrane region M2 and, therefore, this separation seems to be coupled directly to the degree of channel activation.

In order to support and strengthen this model, we have performed electrophysiology experiments on GluR2i(Q)-L483Y receptors, expressed in oocytes. Recently, structures of the GluR2-S1S2 L483Y and N754S (flip) variants, in complexes with a series of compounds, were shown to exhibit degrees of domain closure similar to those of their wild-type (flop) homologues.[42] Although the molecular mechanism for either activation or desensitisation is not fully understood, several studies have suggested that both processes are agonist-dependent.[16,43] Steady-state currents obtained with saturating concentrations of agonists from wild-type receptors differ greatly, indicating a variation in the extent of desensitisation. For example, it has been reported that ACPA desensitises wild-type GluR1o receptors to a lesser extent than AMPA.[44] Qualitatively, we observed the same desensitisation behaviour by ACPA on wild-type GluR2i receptors (data not shown). Using the GluR2i(Q)-L483Y receptor we were able to record peak currents in the absence of desensitisation. The EC_{50} values obtained are comparable to those obtained from GluR1o homomeric receptors.[19,23,31] Moreover, the ranking of the EC_{50} values is the same as that of the IC_{50} values obtained in the [^{3}H]AMPA binding displacement studies. A linear correlation is obtained by comparing the EC_{50} values and the determined IC_{50} values, suggesting that the potency is related directly to the affinity. The obtained rank order of efficacy and the degree of domain closure follow the same trend: 2-Me-Tet-AMPA = ACPA = AMPA = GLU > Br-HIBO. The agonist Br-HIBO, which induces only ca 85% of domain closure compared to the full agonists, elicits only ca 85% of maximal current. Taken together with the structural data, the electrophysiology experiments suggest that the degree of domain closure is coupled directly to the efficacy, and consequently related to channel opening. This is in agreement with observations on kainate[16,45] and on another series of agonists (R.J., T. Banke, M.L.M., S. Traynelis & E.G., unpublished results).

In conclusion, the five GluR2-agonist structures reported here provide the first detailed insight into the molecular basis of ligand–receptor subtype specificity and emphasise the extent to which different ligands utilise distinct binding modes to achieve high-affinity binding. Water molecules associated with the ligand-binding site play a critical role in the mediation of specific ligand–receptor interactions. The GluR2 ligand-binding core adopts distinct conformations depending on the bound ligand and this difference in conformation, in turn, is translated into differential activation of the ion channel. This atomic resolution knowledge of the relationship between the structure of the agonist and the resulting interactions with the receptor can now be employed to understand extant data and to develop new, subtype-selective ligands.

Materials and Methods

Construct design, expression, refolding and purification

The GluR2-S1S2 construct S1S2J was developed by Armstrong & Gouaux.[16] Segment S1 starts at Gly390 and ends at Lys506, whereas S2 starts at Pro632 and ends at Ser775; the two segments are joined by the Gly–Thr linker. The point mutation S1S2J-Y702F was synthesised by the PCR-based method described for the QuickChange Site-directed Mutagenesis Kit (Stratagene) using the following oligonucleotides: PRM1: 5′-AAA TCC AAA GGA AAG TAT GCA T**T**C TTG CTG GAG TCC ACA ATG AAC-3′ and PRM2: 5′-GTT CAT TGT GGA CTC CAG CAA G**A**A TGC ATA CTT TCC TTT GGA TTT-3′. The bold letters correspond to mutated bases. The mutation was verified by double-strand DNA sequencing. The full-length construct GluR2i(Q)-L483Y was developed as described by Chen *et al.*[46] Protein expression, refolding and purification were all done as described.[15]

Activity assay

The agonists (*S*)-ACPA, (*S*)-2-Me-Tet-AMPA and (*S*)-Br-HIBO were synthesised and resolved as described,[20–25] and kindly provided by the members of the Department of Medicinal Chemistry. The [^{3}H]AMPA K_D values were measured for S1S2J and S1S2J-Y702F at pH 7.0 as described.[14] For ligand-binding competition assays on S1S2J and S1S2J-Y702F, the incubations were performed at pH 7.0 in the presence of 20 nM [^{3}H]AMPA (10.6 Ci/mmol) and increasing concentrations of unlabelled agonist. The concentration range was 16 pM–32 μM for (*S*)-ACPA and (*S*)-2-Me-Tet-AMPA, and 68 pM–100 μM for (*S*)-Br-HIBO at S1S2J. The same ranges were used for the S1S2J-Y702F mutant, except for (*S*)-Br-HIBO (0.5 nM–1.8 mM). Ligand-binding experiments were carried out in duplicate.

Oocyte electrophysiology

Two-electrode voltage clamp recordings were performed on oocytes three days after injection of cRNA. Recording was performed using 3 M KCl-filled agarose cushion microelectrodes of resistance 0.5–1.2 MΩ[47] and an amplifier (Axoclamp-2B; Axon Instruments) with an extracellular microelectrode used as the input for a virtual ground bath clamp. The recording chamber had a volume of 5 μl; solutions were applied at 250 μl/min. The extracellular solution contained 100 mM NaCl, 1 mM KCl, 0.5 mM $BaCl_2$, 1.0 mM $MgCl_2$, and 5 mM Hepes (pH 7.5). Agonists were applied for 15 seconds every 90 seconds. A holding potential of −60 mV was used. Responses were corrected for run down when necessary. Data were processed and analysed using the programs Synapse and KaleidaGraph.

Co-crystallisation of S1S2J and S1S2J-Y702F with ligands

A 10 mg/ml preparation (as determined by $A_{280} \cong 1$ mg/ml) of S1S2J or of the S1S2J-Y702F mutant in 10 mM Hepes (pH 7.0), 20 mM NaCl, 1 mM EDTA was used for crystallisation. Final ligand concentrations for the S1S2J and S1S2J-Y702F complexes were: 3 mM (*S*)-ACPA and (*S*)-2-Me-Tet-AMPA, and 8 mM (*S*)-Br-HIBO. Crystals were grown at 4 °C in hanging drops containing a 1:1 (v/v) ratio of protein and precipitant solution. S1S2J:ACPA, S1S2J-Y702F:ACPA, and S1S2J:2-Me-Tet-AMPA co-crystals grew using a reservoir solution composed of 12–18% (w/v) PEG 8000, 0.15–0.28 M zinc acetate, and 0.1 M sodium cacodylate at pH 6.5. S1S2J:Br-HIBO crystallisation buffer contained 18–23% PEG 1450, 0.2–0.27 M Li_2SO_4, and 0.1 M phosphate-citrate (pH 4.5). S1S2J-Y702F:Br-HIBO crystals grew under conditions identical with that for S1S2J:Br-HIBO, except that 15–20% PEG 3350 replaced PEG 1450. The reservoir volume was 0.5 ml. Crystals grew to an average size of 0.15 mm × 0.05 mm × 0.06 mm within a week. The crystals were transferred into crystallisation buffer with the corresponding ligand and 12–18% glycerol as a cryoprotectant before being flash-cooled in liquid nitrogen.

X-ray data collection

Data for S1S2J:2-Me-Tet-AMPA were collected on an R-Axis IV image plate system, using Cu Kα radiation at Columbia University (USA). Synchrotron data for S1S2J:ACPA were collected on the EMBL beamline BW7B at the DORIS storage ring, DESY, Hamburg, using a MAR IP detector and the S1S2J:Br-HIBO data on a MAR CCD detector at beamline BW7A. Synchrotron data for S1S2J-Y702F:ACPA and S1S2J-Y702F:HIBO were collected on the EMBL, Hamburg, beamline X11 and X13, respectively, both using MAR CCD detectors. All data were collected at 110 K. Data processing was performed using DENZO, Scalepack,[48] and the CCP4 suite of programs.[49] For further details, see Table 1.

Structure refinements

The S1S2J:2-Me-Tet-AMPA structure was determined by difference Fourier using phases calculated from the structure of S1S2J:AMPA (PDB ID code 1FTM, protomer A, without water molecules and ligand).[16] The first refinement protocol (p1), using strict non-crystallographic symmetry (NCS), began with rigid-body refinement and maximum-likelihood refinement in CNS version 0.5.[50] Following model building in program O version 6.2.1,[51] restrained NCS was applied during the second refinement protocol (p2), consisting of maximum-likelihood refinement and individual *B*-factors refinement. NCS restraints were released completely in the third refinement cycle. The R_{free} value converged after a number of interchanging cycles of model building (including addition of waters, ligands and Zn ions) and refinement, according to protocol (p2).

The structure of S1S2J:Br-HIBO was determined by molecular replacement (MR) using AMoRe[52] with the structure of S1S2J:2-Me-Tet-AMPA (protomer A, without water molecules or ligand) as a search model. A clear solution was found in the cross-rotation functions and subsequent translation function (CC = 51.40, $R_{fac} = 44.0\%$). These values were improved after 30 cycles of rigid-body refinement using AMoRe (CC = 68.0, $R_{fac} = 37.9\%$). Automatic model building was performed with the program ARP/wARP version 5.1[53] using the phases from the MR solution. The warpNtrace procedure within ARP/wARP automatically built 97% of the residues. The model was completed after three cycles of manual rebuilding (including addition of water molecules and ligand) and refinement using CNS version 1.0. The data set of S1S2J:ACPA was phased using the structure of protomer A from S1S2J:2-Me-Tet-AMPA, excluding water molecules and the ligand. The structures of S1S2J-Y702F:ACPA and S1S2J-Y702F:Br-HIBO were determined by difference Fourier using phases calculated from the structure of S1S2J:ACPA and S1S2J:Br-HIBO, respectively. The initial models were refined according to the same procedure as that used for S1S2J:Br-HIBO. That is, the structures were partly built and refined using ARP/wARP, manually rebuilt and refined in CNS.

The ligand molecules in all complexes could be placed unambiguously into the $F_o - F_c$ map. In order to obtain reliable bond lengths and bond angles, the ligands were initially geometry optimised using the semi-empirical method AM1 implemented in Spartan version 5.1.1 (Wavefunction Inc., Irvine, CA, 1991–1998). The calculations were performed in presence of the SM2 solvation model. Topology and parameter files included in the crystallographic refinement program CNS and in program O were generated by the HIC-Up server.[54] All structures were refined using the data from the highest to the lowest-resolution bin during the whole refinement procedure. The final refinement statistics are shown in Table 2.

Protein Data Bank accession numbers

Coordinates of the final structures have been deposited in RCSB Protein Data Bank (1M5B-F).

Acknowledgments

We thank Lotte Brehm, Stine B. Vogensen, Ulf Madsen, and Povl Krogsgaard-Larsen for generously supplying us with (*S*)-2-Me-Tet-AMPA, (*S*)-ACPA, and (*S*)-Br-HIBO. We are grateful to Neali Armstrong and Rich Olson for advice and helpful assistance. Jeremy R. Greenwood is thanked for discussion and guidance using computational techniques. Victor S. Lamzin is thanked for assistance with the program ARP/wARP and Willy R. Wriggers with the HINGEFIND script. The work was supported by grants from NeuroScience PharmaBiotec; DANSYNC (Danish Centre for Synchrotron Based Research); European Community—access to Research Infrastructure Action of the Improving Human Potential Programme to the EMBL Hamburg Outstation, contract number: HPRI-CT-1999-00017; Novo Nordisk Fonden; Apotekerfonden af 1991; and the Danish Medical Research Council. Work in the Gouaux laboratory on glutamate receptors is supported by grants from NIH and NARSAD. E. Gouaux is a Klingenstein Fellow and an assistant investigator of the Howard Hughes Medical Institute.

References

1. Dingledine, R., Borges, K., Bowie, D. & Traynelis, S. F. (1999). The glutamate receptor ion channels. *Pharmacol. Rev.* **51**, 7–61.
2. Hollmann, M. & Heinemann, S. (1994). Cloned glutamate receptors. *Annu. Rev. Neurosci.* **17**, 31–108.
3. Borges, K. & Dingledine, R. (1998). AMPA receptors: molecular and functional diversity. *Prog. Brain Res.* **116**, 153–170.
4. Seeburg, P. H. (1996). The role of RNA editing in controlling glutamate receptor channel properties. *J. Neurosci.* **66**, 1–5.
5. Seeburg, P. H. (1993). The TINS/TIPS lecture. The molecular biology of mammalian glutamate receptor channels. *Trends Neurosci.* **16**, 359–365.
6. Hollmann, M., Maron, C. & Heinemann, S. (1994). N-Glycosylation site tagging suggests a three transmembrane domain topology for the glutamate receptor GluR1. *Neuron*, **13**, 1331–1343.
7. Stern-Bach, Y., Bettler, B., Hartley, M., Sheppard, P. O., O'Hara, P. J. & Heinemann, S. F. (1994). Agonist selectivity of glutamate receptors is specified by two domains structurally related to bacterial amino acid-binding proteins. *Neuron*, **13**, 1345–1357.
8. Wo, Z. G. & Oswald, R. E. (1994). Transmembrane topology of two kainate receptor subunits revealed by N-glycosylation. *Proc. Natl Acad. Sci. USA*, **91**, 7154–7158.
9. Bennett, J. A. & Dingledine, R. (1995). Topology profile for a glutamate receptor: three transmembrane domains and a channel-lining reentrant membrane loop. *Neuron*, **14**, 373–384.
10. O'Hara, P. J., Sheppard, P. O., Thogersen, H., Venezia, D., Haldeman, B. A., McGrane, V. *et al.* (1993). The ligand-binding domain in metabotropic glutamate receptors is related to bacterial periplasmic binding proteins. *Neuron*, **11**, 41–52.
11. Nakanishi, N., Shneider, N. A. & Axel, R. (1990). A family of glutamate receptor genes: evidence for the formation of heteromultimeric receptors with distinct channel properties. *Neuron*, **5**, 569–581.
12. Armstrong, N., Sun, Y., Chen, G.-Q. & Gouaux, E. (1998). Structure of a glutamate receptor ligand binding core in complex with kainate. *Nature*, **395**, 913–917.
13. Kuusinen, A., Arvola, M. & Keinänen, K. (1995). Molecular dissection of the agonist binding site of an AMPA receptor. *EMBO J.* **14**, 6327–6332.
14. Chen, G.-Q. & Gouaux, E. (1997). Overexpression of a glutamate receptor (GluR2) ligand binding domain in *Escherichia coli*: application of a novel protein folding screen. *Proc. Natl Acad. Sci. USA*, **94**, 13431–13436.
15. Chen, G.-Q., Sun, Y., Jin, R. & Gouaux, E. (1998). Probing the ligand binding domain of the GluR2 receptor by proteolysis and deletion mutagenesis defines domain boundaries and yields a crystallizable construct. *Protein Sci.* **7**, 2623–2630.
16. Armstrong, N. & Gouaux, E. (2000). Mechanisms for activation and antagonism of an AMPA-sensitive glutamate receptor: crystal structures of the GluR2 ligand binding core. *Neuron*, **28**, 165–181.
17. Bräuner-Osborne, H., Egebjerg, J., Nielsen, E.Ø., Madsen, U. & Krogsgaard-Larsen, P. (2000). Ligands for glutamate receptors: design and therapeutic prospects. *J. Med. Chem.* **43**, 2609–2645.
18. Coquelle, T., Christensen, J. K., Banke, T. G., Madsen, U., Schousboe, A. & Pickering, D. S. (2000). Agonist discrimination between AMPA receptor subtypes. *Neuroreport*, **11**, 2643–2648.
19. Banke, T. G., Greenwood, J. R., Christensen, J. K., Liljefors, T., Traynelis, S. F., Schousboe, A. & Pickering, D. S. (2001). Identification of amino acid residues in GluR1 responsible for ligand binding and desensitization. *J. Neurosci.* **21**, 3052–3062.
20. Madsen, U. & Wong, E. H. F. (1992). Heterocyclic excitatory amino acids. Synthesis and biological activity of novel analogues of AMPA. *J. Med. Chem.* **35**, 107–111.
21. Johansen, T. N., Stensbøl, T. B., Nielsen, B., Vogensen, S. B., Frydenvang, K., Sløk, F. A. *et al.* (2001). Resolution, configurational assignment, and enantiopharmacology at glutamate receptors of 2-amino-3-(3-carboxy-5-methyl-4-isoxazolyl)propionic acid (ACPA) and demethyl-ACPA. *Chirality*, **13**, 523–532.
22. Bang-Andersen, B., Lenz, S. M., Skjærbæk, N., Søby, K. K., Hansen, H. O., Ebert, B. *et al.* (1997). Heteroaryl analogues of AMPA. Synthesis and quantitative structure–activity relationships. *J. Med. Chem.* **40**, 2831–2842.
23. Vogensen, S. B., Jensen, H. S., Stensbøl, T. B., Frydenvang, K., Bang-Andersen, B., Johansen, T. N. *et al.* (2000). Resolution, configurational assignment, and enantiopharmacology of 2-amino-3-[3-hydroxy-5-(2-methyl-2*H*-tetrazol-5-yl)isoxazol-4-yl]propionic acid, a potent GluR3- and GluR4-preferring AMPA receptor agonist. *Chirality*, **12**, 705–713.
24. Krogsgaard-Larsen, P., Honoré, T. & Hansen, J. J. (1980). New class of glutamate agonist structurally related to ibotenic acid. *Nature*, **284**, 64–66.
25. Hansen, J. J., Nielsen, B., Krogsgaard-Larsen, P., Brehm, L., Nielsen, E.Ø. & Curtis, D. R. (1989). Excitatory amino acid agonists. Enzymic resolution, X-ray structure, and enantioselective activities of (*R*)- and (*S*)-bromohomoibotenic acid. *J. Med. Chem.* **32**, 2254–2260.
26. Bleakman, D. & Lodge, D. (1998). Neuropharmacology of AMPA and kainate receptors. *Neuropharmacology*, **37**, 1187–1204.
27. Keinänen, K., Wisden, W., Sommer, B., Werner, P., Herb, A., Verdoorn, T. A. *et al.* (1990). A family of AMPA-selective glutamate receptors. *Science*, **249**, 556–560.
28. Wriggers, W. & Schulten, K. (1997). Protein domain movements: detection of rigid domains and visualization of hinges in comparisons of atomic coordinates. *Proteins*, **29**, 1–14.
29. Humphrey, W., Dalke, A. & Schulten, K. (1996). VMD—visual molecular dynamics. *J. Mol. Graph.* **14**, 33–38.
30. Stern-Bach, Y., Russo, S., Neuman, M. & Rosenmund, C. (1998). A point mutation in the glutamate binding site blocks desensitization of AMPA receptors. *Neuron*, **21**, 907–918.
31. Banke, T. G., Schousboe, A. & Pickering, D. S. (1997). Comparison of the agonist binding site of homomeric, heteromeric, and chimeric GluR1o and GluR3o AMPA receptors. *J. Neurosci. Res.* **49**, 176–185.
32. Madsen, U., Frølund, B., Lund, T. M., Ebert, B. & Krogsgaard-Larsen, P. (1993). Design, synthesis and pharmacology of model compounds for indirect elucidation of the topography of AMPA receptor sites. *Eur. J. Med. Chem.* **28**, 791–800.
33. Sløk, F. A., Ebert, B., Lang, Y., Krogsgaard-Larsen, P., Lenz, S. M. & Madsen, U. (1997). Excitatory amino-acid receptor agonists. Synthesis and pharmacology

of analogues of 2-amino-3-(3-hydroxy-5-methylisoxazol-4-yl)propionic acid. *Eur. J. Med. Chem.* **32**, 329–338.
34. Falch, E., Brehm, L., Mikkelsen, I., Johansen, T. N., Skjærbæk, N., Nielsen, B. *et al.* (1998). Heteroaryl analogues of AMPA. 2. Synthesis, absolute stereochemistry, photochemistry, and structure–activity relationships. *J. Med. Chem.* **41**, 2513–2523.
35. Christensen, I. T., Ebert, B., Madsen, U., Nielsen, B., Brehm, L. & Krogsgaard-Larsen, P. (1992). Excitatory amino acid receptor ligands. Synthesis and biological activity of 3-isoxazolol amino acids structurally related to homoibotenic acid. *J. Med. Chem.* **35**, 3512–3519.
36. Greenwood, J. R., Vaccarella, G., Capper, H. R., Allan, R. D. & Johnston, G. A. R. (1998). Heterocycles as bioisosteres for the ω-carboxylate moiety of glutamate in AMPA receptor agonists: a review and theoretical study. *Internet J. Chem.* **1**, 38 http://www.ijc.com.
37. Johansen, T. N., Ebert, B., Falch, E. & Krogsgaard-Larsen, P. (1997). AMPA receptor agonists: resolution, configurational assignment, and pharmacology of (+)-(*S*)- and (−)-(*R*)-2-amino-3-[3-hydroxy-5-(2-pyridyl)isoxazol-4-yl]propionic acid (2-Py-AMPA). *Chirality*, **9**, 274–280.
38. Bang-Andersen, B. (1996). Synthesis and structure–activity relationships. PhD Thesis. The Royal Danish School of Pharmacy, Copenhagen
39. Kromann, H., Sløk, F. A., Stensbøl, T. B., Bräuner-Osborne, H., Madsen, U. & Krogsgaard-Larsen, P. (2002). Selective antagonists at group I metabotropic glutamate receptors: synthesis and molecular pharmacology of 4-aryl-3-isoxazolol amino acids. *J. Med. Chem.* **45**, 988–991.
40. Swanson, G. T., Gereau, R. W., Green, T. & Heinemann, S. F. (1997). Identification of amino acid residues that control functional behavior in GluR5 and GluR6 kainate receptors. *Neuron*, **19**, 913–926.
41. Mayer, M. L., Olson, R. & Gouaux, E. (2001). Mechanisms for ligand binding to GluR0 ion channels: crystal structures of the glutamate and serine complexes and a closed apo state. *J. Mol. Biol.* **311**, 815–836.
42. Sun, Y., Olson, R., Horning, M., Armstrong, N., Mayer, M. & Gouaux, E. (2002). Mechanism of glutamate receptor desensitization. *Nature*, **417**, 245–253.
43. Paas, Y. (1998). The macro- and microarchitectures of the ligand-binding domain of glutamate receptors. *Trends Neurosci.* **21**, 117–125.
44. Wahl, P., Madsen, U., Banke, T., Krogsgaard-Larsen, P. & Schousboe, A. (1996). Different characteristics of AMPA receptor agonists acting at AMPA receptors expressed in Xenopus oocytes. *Eur. J. Pharmacol.* **308**, 211–218.
45. Koike, M., Tsukada, S., Tsuzuki, K., Kijima, H. & Ozawa, S. (2000). Regulation of kinetic properties of GluR2 AMPA receptor channels by alternative splicing. *J. Neurosci.* **20**, 2166–2174.
46. Chen, G.-Q., Cui, C., Mayer, M. L. & Gouaux, E. (1999). Functional characterization of a potassium-selective prokaryotic glutamate receptor. *Nature*, **402**, 817–821.
47. Schreibmayer, W., Lester, H. A. & Dascal, N. (1994). Voltage clamping of *Xenopus laevis* oocytes utilizing agarose-cushion electrodes. *Pflügers Arch.* **426**, 453–458.
48. Otwinowski, Z. & Minor, W. (1997). Processing of X-ray diffraction data collected in oscillation mode. *Methods Enzymol.* **276**, 307–326.
49. Collaborative Computational Project Number 4 (1994). The CCP4 suite: programs for protein crystallography. *Acta Crystallog. sect. D*, **50**, 760–763.
50. Brünger, A. T., Adams, P. D., Clore, G. M., DeLano, W. L., Gros, P., Grosse-Kunstleve, R. W. *et al.* (1998). Crystallography & NMR system: a new software suite for macromolecular structure determination. *Acta Crystallog. sect. D*, **54**, 905–921.
51. Jones, T. A., Zou, J. Y., Cowan, S. W. & Kjeldgaard, M. (1991). Improved methods for binding protein models in electron density maps and the location of errors in these models. *Acta Crystallog. sect. A*, **47**, 110–119.
52. Navaza, J. (1994). AMoRe: an automated package for molecular replacement. *Acta Crystallog. sect. A*, **50**, 157–163.
53. Perrakis, A., Morris, R. & Lamzin, V. S. (1999). Automated protein model building combined with iterative structure refinement. *Nature Struct. Biol.* **6**, 458–463.
54. Kleywegt, G. J. & Jones, T. A. (1998). Databases in protein crystallography. *Acta Crystallog. sect. D*, **54**, 1119–1131.
55. Wallace, A. C., Laskowski, R. A. & Thornton, J. M. (1995). LIGPLOT: a program to generate schematic diagrams of protein–ligand interactions. *Protein Eng.* **8**, 127–134.
56. Esnouf, R. M. (1997). An extensively modified version of Molscript that includes greatly enhanced coloring capabilities. *J. Mol. Graph. Model.* **15**, 132–134.
57. Kraulis, P. J. (1991). Molscript: a program to produce both detailed and schematic plots of protein structures. *J. Appl. Crystallog.* **24**, 946–950.
58. Merritt, E. A. & Murphy, M. E. P. (1994). Raster3D version 2.0. A program for photorealistic molecular graphics. *Acta Crystallog. sect. D*, **50**, 869–873.
59. Kleywegt, G. J. & Jones, T. A. (1996). Phi/Psi-chology: Ramachandran revisited. *Structure*, **4**, 1395–1400.

Edited by R. Huber

(Received 1 March 2002; received in revised form 14 June 2002; accepted 21 June 2002)